Infrared Characterization of the HCOOH···CO 2 Complexes in Solid Argon: Stabilization of the Higher-Energy Conformer of Formic Acid

ARTICLE *in* THE JOURNAL OF PHYSICAL CHEMISTRY A · MAY 2012

Impact Factor: 2.69 · DOI: 10.1021/jp302911p · Source: PubMed

4 AUTHORS, INCLUDING:

Masashi Tsuge
National Chiao Tung University
21 PUBLICATIONS **119** CITATIONS
SEE PROFILE

Markku Rasanen
University of Helsinki
268 PUBLICATIONS **7,058** CITATIONS
SEE PROFILE

THE JOURNAL OF PHYSICAL CHEMISTRY A

Article

pubs.acs.org/JPCA

Infrared Characterization of the HCOOH···CO_2 Complexes in Solid Argon: Stabilization of the Higher-Energy Conformer of Formic Acid

Masashi Tsuge,* Kseniya Marushkevich, Markku Räsänen, and Leonid Khriachtchev*

Department of Chemistry, University of Helsinki, P.O. Box 55, FIN-00014, Finland

Supporting Information

ABSTRACT: The complexes of formic acid (HCOOH, FA) with carbon dioxide are studied by infrared spectroscopy in an argon matrix. Two *trans*-FA···CO_2 and one *cis*-FA···CO_2 complexes are experimentally identified while the calculations at the MP2(full)/6-311++G(2d,2p) level of theory predict one more minimum for the *cis*-FA···CO_2 complex. The complex of the higher-energy conformer *cis*-FA with CO_2 is prepared by vibrational excitation of the ground-state *trans*-FA conformer combined with thermal annealing. The lifetime of the *cis*-FA···CO_2 complex in an argon matrix at 10 K is 2 orders of magnitude longer than that of the *cis*-FA monomer. This big difference is explained by the computational results which show a higher stabilization barrier for the complex. The solvation effects in solid argon are theoretically estimated and their contribution to the stabilization barriers of the higher-energy species is discussed. The relative barrier transmissions for hydrogen tunneling in the *cis*-FA···CO_2 complex and *cis*-FA monomer are in good agreement with the experimental decay rates.

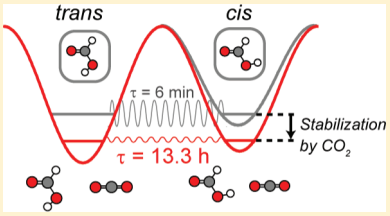

INTRODUCTION

Hydrogen bonding and conformational isomerism are important phenomena in many branches of science. The O−H···O and C−H···O hydrogen bonds play crucial roles in determining properties of matter and molecular conformation is a key concept in the selectivity and functionality of biologically active molecules.[1] Many conformational changes, which involve a movement of hydrogen, are known to proceed via quantum tunneling at low-temperatures,[2−5] and it has been shown that the quantum tunneling also contributes to the chemical reaction involving movements of a heavier atom (carbon and oxygen).[6] Moreover, quantum tunneling can change a reaction to the opposite direction compared to the classical view.[7] The importance of quantum tunneling for low-temperature chemistry in the interstellar ices should be also mentioned.[8−10]

Formic acid (HCOOH, FA) is the smallest organic acid that has conformational isomerism which proceeds via quantum tunneling of the O−H hydrogen atom.[11] The trans and cis conformers of FA can form a variety of hydrogen bonds. The amount of the *cis*-FA form is very small under normal conditions, because *cis*-FA is higher in energy than *trans*-FA by ∼1365 cm^{-1}.[12] The *cis*-FA conformer can be prepared in large amounts by vibrational excitation of *trans*-FA in low temperature matrices.[11,13−15] This method has been proven to be a powerful tool to study conformational changes in cryogenic matrices, in particular, conformation-dependent reactions. In fact, a conformation-dependent reaction between FA and oxygen atom has been found where the formation of peroxyformic acid (HCOOOH) occurs only from *trans*-FA.[16] Understanding environmental effects on conformation-dependent reactions is an interesting task which has not been sufficiently addressed.

It has been found that the cis-to-trans FA conversion rate strongly depends on the matrix material, isotopic substitutions, matrix temperature, and interaction with other molecules.[11,15−26] Hydrogen tunneling is completely suppressed when *cis*-FA forms complexes with O atom and H_2O,[16,20] or in some of the trans−cis dimers, where strong hydrogen bonds are formed.[24] A substantial decrease of hydrogen tunneling rate is also observed for the trans−cis dimers where the tunneling hydrogen atom of *cis*-FA does not participate in intermolecular bonding,[22,23] or for relatively weak hydrogen bond such as in the complex with N_2.[21] This shows that intermolecular interaction can control the stabilization barrier of the *cis*-FA conformer. Thus, it is interesting to study more complexes of *cis*-FA in order to correlate this stabilization effect with the strength of the intermolecular interaction.

In the present work, we study, both experimentally and theoretically, the FA···CO_2 complexes. These complexes are characterized by using infrared spectroscopy in an argon matrix with the aid of ab initio calculations. Tunneling decay of the *cis*-FA···CO_2 complex is measured and discussed based on the estimate of the stabilization barrier. The effect of an argon matrix is also estimated. The FA···CO_2 complexes are of particular interest due to the existence of these species not only on Earth but also in interstellar, cometary, and planetary ices and dust.[27] FA complexes with CO_2 can also be of interest in H_2 storage systems, where H_2 and CO_2 react with a catalyst producing FA in water solutions.[28]

Received: March 27, 2012
Revised: May 7, 2012
Published: May 7, 2012

COMPUTATIONAL DETAILS AND RESULTS

Computational Details. The quantum chemical calculations were performed using Gaussian 09 program.[29] The equilibrium geometry and vibrational frequencies of *trans*- and *cis*-FA monomers and the FA···CO_2 complexes were calculated at the MP2(full)/6-311++G(2d,2p) level of theory. This level of theory has been used for the calculations of FA dimers and FA···N_2 complexes and it reproduces well the experimental vibrational properties.[21−25] The geometry optimizations were done with the tight convergence criteria. The optimized structures were verified to be true minima on the basis of the harmonic vibrational analysis, which yielded no imaginary frequencies. The interaction energies of the complexes were calculated as the difference between the total energies of the complexes and the monomers (with the geometry in the complexes). The basis set superposition error (BSSE) was corrected by the counterpoise method.[30] The zero-point energies were also accounted for using the calculated harmonic frequencies.

The cis-to-trans conversion barriers were calculated by scanning the torsional angle from 0° (*trans*-FA) to 180° (*cis*-FA). In this procedure, the coordinates of all the atoms excluding the tunneling hydrogen were frozen, which corresponds to the adiabatic approximation when the heavy atoms do not move during the fast hydrogen tunneling.[31] In this scan, the zero-point energy correction was not used because one cannot calculate vibrational frequencies for nonstationary points.

The solvation energies of the monomers and complexes in solid argon were estimated by the polarizable continuum model (PCM) at the MP2(full)/6-311++G(2d,2p) level of theory using the structures optimized in vacuum.[32]

Computational Results. Two planar *trans*-FA···CO_2 structures are found (complexes **I** and **II** in Figure 1). Complex **I** is stabilized by an O−H···O hydrogen bond (length of 2.04 Å) and complex **II** is most probably stabilized by dispersion and electrostatic (dipole−quadrupole interaction) forces. The interaction energies of complexes **I** and **II** are −9.89 and −5.45 kJ mol^{-1}, respectively. For the *cis*-FA···CO_2 system, one planar and one nonplanar structures are found (complexes **III** and **IV** in Figure 1). The more stable complex **III** is stabilized by an O−H···O hydrogen bond (length of 2.05 Å) and has an interaction energy of −8.54 kJ mol^{-1}. In structure **IV**, CO_2 makes an angle of 62.9° with the FA plane. This complex with an interaction energy of −6.71 kJ mol^{-1} is presumably stabilized by dispersion and electrostatic forces.

The harmonic frequencies for the characteristic modes are given in Tables 1 and 2. The frequency shifts are calculated as the difference between the frequencies of the complexes and monomers. For complexes **I** and **III**, the most significant shifts are predicted for the OH stretching (νOH) and COH torsional (τCOH) modes. The red shift of νOH and blue shift of τCOH are caused by the formation of the O−H···O hydrogen bonds. For complexes **II** and **IV**, all the predicted shifts are less than 10 cm^{-1}.

The cis-to-trans torsional barrier calculated for the *cis*-FA monomer and *cis*-FA···CO_2 complex **III** are shown in Figure 2. The barrier heights, which are defined as the energy difference between the transition state and the cis conformation, are 3242 cm^{-1} for the *cis*-FA monomer and 4161 cm^{-1} for the *cis*-FA···CO_2 complex **III** (BSSE corrected). For complex **IV**, the stabilization barrier is 3205 cm^{-1}, i.e. close to that of the monomer. The solvation energies calculated for the *cis*-FA monomer and its transition state are −1077 and −951 cm^{-1}, respectively, and those for the *cis*-FA···CO_2 complex **III** and its transition state are −934 and −1112 cm^{-1}. As a result, the barrier in solid argon becomes 126 cm^{-1} (~5%) higher for the *cis*-FA monomer and 178 cm^{-1} (~7%) lower for complex **III** as compared with the corresponding barriers in vacuum. For complex **IV**, the stabilization barrier does not change much by solvation (3184 cm^{-1}).

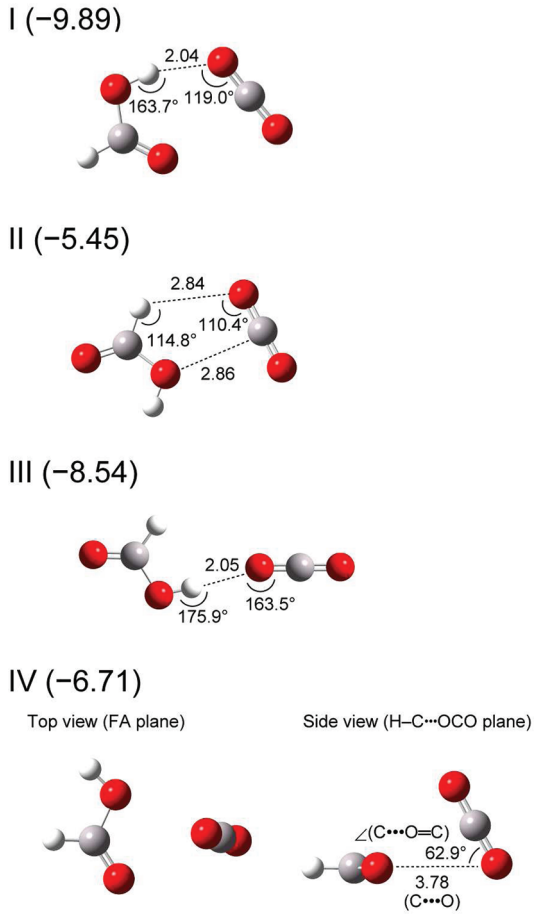

Figure 1. Structures of the *trans*-FA···CO_2 (**I** and **II**) and *cis*-FA···CO_2 (**III** and **IV**) complexes optimized at the MP2(full)/6-311++G(2d,2p) level of theory. The interaction energies (in kJ mol^{-1}) are given in parentheses. Bond lengths are in Å.

EXPERIMENTAL DETAILS AND RESULTS

Experimental Details. The gaseous mixtures of FA (Kebo Lab, 99%), carbon dioxide (AGA, 99.995%), and argon (AGA, 99.9999%) were prepared by standard manometric procedures. Formic acid was degassed by several freeze−pump−thaw cycles. The gas mixture (FA:CO_2:Ar = 1:8:1000) was deposited onto a CsI substrate kept at 10 K in a closed-cycle helium cryostat (APD, DE 202A). The IR spectra were measured using an FTIR spectrometer (Bruker, Vertex 80v) with 1 cm^{-1} resolution coadding 200 scans. For the kinetic measurements, a long-pass filter that transmits below 1850 cm^{-1} was inserted between the Globar source and the cryostat in order to eliminate the light-induced cis-to-trans conversion.[15] The Globar light was blocked between the measurements. Conformational changes were promoted by an optical parametric oscillator (OPO Sunlite with an IR extension,

dx.doi.org/10.1021/jp302911p | J. Phys. Chem. A 2012, 116, 5305−5311

Table 1. Experimental and Computational Frequencies and Shifts (in cm^{-1}) for the Characteristic Vibrational Modes of the *trans*-FA and CO_2 Monomers and *trans*-FA···CO_2 Complexes I and II[a,b,c]

	trans-FA, exptl[d]	monomers, calcd	I, exptl	shift I, exptl	I, calcd	shift I, calcd	II, exptl	shift II, exptl	II, calcd	shift II, calcd
νOH	3550.0	3783.9 (83)	3505.0	−45.0	3726.2 (265)	−57.7	3546.0	−4.0	3781.5 (84)	−2.4
CO_2 asym stretch		2403.0 (587)			2405.6 (574)	+2.6			2405.2 (550)	+2.2
νC═O	1767.5	1788.7 (335)	1755.4	−12.1	1776.6 (307)	−12.1	1761.7	−5.8	1789.6 (344)	+0.9
CO_2 sym stretch		1320.5 (0)			1322.1 (3)	+1.6			1322.3 (0)	+1.8
CO−COH def	1305.6[e]	1316.9 (9)	1280.0		1348.0 (12)	+20.3			1307.8 (6)	−9.1
	1215.4[e]		1276.5							
			1274.7							
			1272.3							
COH−CO def	1103.6	1123.4 (284)	1125.8	+22.2	1153.6 (249)	+30.2	[1099.2][f]	[−4.4][f]	1114.1 (268)	−9.1
CO_2 bend		665.6 (22)			664.0 (17)	−1.6			666.9 (5)	+1.3
τCOH	635.4	676.6(144)	689.4	+54.0	757.9 (122)	+81.3	628.2	−7.2	657.8 (155)	−0.8

[a]Computations were done at the MP2(full)/6-311++G(2d,2p) level of theory. [b]Shift is the difference between the complex and monomer frequencies. [c]Infrared intensities (in km mol^{-1}) are given in the parentheses. [d]FA in site 2.[33] [e]Fermi resonance doublet between the CO−COH def. fundamental and the first overtone of τCOH. [f]Tentative assignments.

Table 2. Experimental and Computational Frequencies and Shifts (in cm^{-1}) for the Characteristic Vibrational Modes of the *cis*-FA and CO_2 Monomers and *cis*-FA···CO_2 Complexes III and IV[a,b,c]

	cis-FA, exptl[d]	monomers, calcd	III, exptl	shift III, exptl	III, calcd	shift III, calcd	IV, calcd	shift IV, calcd
νOH	3615.9	3851.2 (83)	3600.5	−15.4	3833.2 (363)	−18.0	3849.1 (90)	−2.1
CO_2 asym stretch		2403.0 (587)			2412.3 (715)	+9.3	2405.5 (543)	+2.5
νC═O	1806.9	1829.0(269)	1800.2	−6.7	1824.1 (328)	−4.9	1825.0 (245)	−4.0
CO_2 sym stretch		1320.5 (0)			1328.4 (8)	+7.9	1322.7 (0)	+2.2
CO−COH def	1248.7	1287.1(297)	1277.2	+28.5	1320.1 (270)	+33.0	1285.3 (286)	−1.8
			1274.7	+26.0				
			1258.3	+8.4				
			1256.4	+7.7				
			1251.6	+2.9				
			1249.7	+1.0				
			1245.3	−3.4				
COH−CO def	1107.0	1113.0 (79)			1132.5 (105)	+19.5	1113.9 (71)	+0.9
CO_2 bend		665.6 (22)			659.3 (21)	−6.3	663.3 (22)	−2.3
τCOH	504.8	536.6(89)	565.5	+60.7	625.5 (83)	+88.9	527.4 (83)	−6.2
			557.8	+53.0				

[a]Computations were done at the MP2(full)/6-311++G(2d,2p) level of theory. [b]Shift is the difference between the complex and monomer frequencies. [c]Infrared intensities (in km mol^{-1}) are given in the parentheses. [d]FA in site 2.[33]

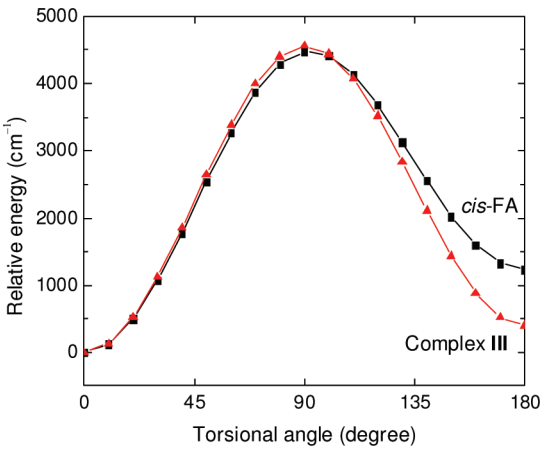

Figure 2. Calculated torsional barriers for the cis-to-trans conversion of the *cis*-FA monomer (squares) and *cis*-FA···CO_2 complex **III** (triangles) in vacuum. The BSSE are corrected for the complex. The torsional angles of 0° and 180° correspond to the *trans*- and *cis*-FA conformations, respectively.

Continuum) that produces IR light with a pulse duration of 5 ns, line width of 0.1 cm^{-1}, and repetition rate of 10 Hz. A Burleigh WA-4500 wavemeter was used to measure the OPO signal frequency, providing accuracy better than 1 cm^{-1} for the difference frequency.

Experimental Results. Figure 3 presents the IR spectra measured for an FA:CO_2:Ar = 1:8:1000 matrix. In the C═O stretching region, two CO_2-induced bands are observed at 1755.4 and 1761.7 cm^{-1} after deposition at 10 K (marked with I and II), together with the known absorptions of the *trans*-FA monomer (1767.5 and 1765.0 cm^{-1}) and *trans*-FA dimers (tt1, 1728 cm^{-1}; tt2, 1746 cm^{-1}) (trace 1).[23,33] A weak absorption of the *cis*-FA monomer is seen at 1806.9 cm^{-1}. In the deformation region, four CO_2-induced bands (marked with I) are observed at 1280.0, 1276.5, 1274.7, and 1272.3 cm^{-1}, together with the Fermi resonance doublet of the *trans*-FA monomer at 1215.4 and 1305.6 cm^{-1}, and the *cis*-FA monomer bands at 1248.7 and 1243.4 cm^{-1}.[33] Upon annealing at 30 K, a number of bands of the *trans*-FA···CO_2 complex increase (group I) and some of CO_2-induced bands disappear (group II) (trace 2 in Figure 3).

dx.doi.org/10.1021/jp302911p | J. Phys. Chem. A 2012, 116, 5305−5311

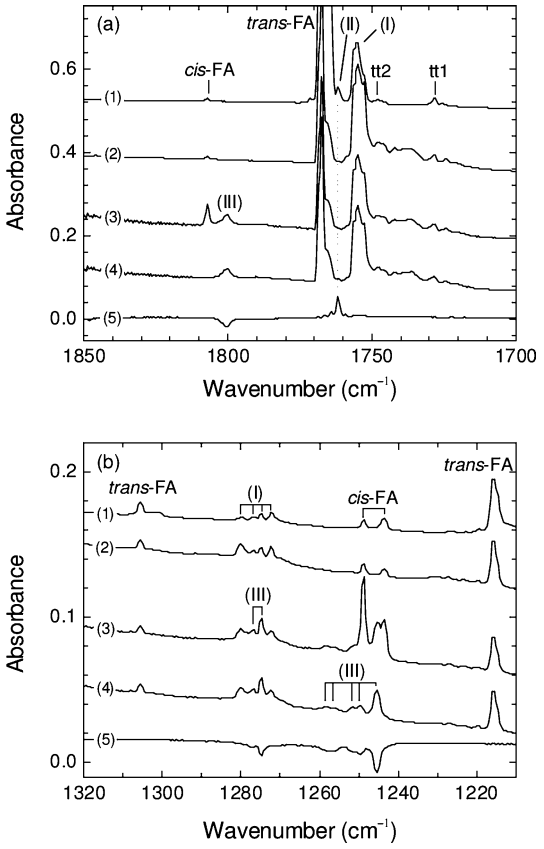

Figure 3. FTIR spectra in (a) C═O stretching and (b) CO−COH deformation regions measured for HCOOH:CO_2:Ar = 1:8:1000. (1) After deposition at 10 K, (2) after annealing at 30 K, (3) after annealing at 30 K during excitation at 3550 cm^{-1}, (4) 1 h after trace 3, and (5) 19 h after trace 4 (difference spectrum). Spectra 1 and 2 are measured without a long-pass filter and spectra 3−5 are measured with a long-pass filter. The spectra were measured at 10 K.

The CO_2-induced bands are shown in Table 1, and they presumably originate from the *trans*-FA···CO_2 complexes.

Excitation of the νOH mode of *trans*-FA at 3550 cm^{-1} produces *cis*-FA molecules in large amounts.[13−15] If the matrix is annealed during this excitation, a new band III at 1800.2 cm^{-1} appears in the C═O stretching region (trace 3 in Figure 3). In the deformation region, the corresponding bands are at 1258.3, 1256.4, 1251.6, 1249.7, and 1245.3 cm^{-1}. The relative intensities of four bands around 1275 cm^{-1} are different from those in trace 2. Thus, the 1277.2 and 1274.7 cm^{-1} bands are probably contributed by the presence of *cis*-FA. These seven bands in the deformation region seem to arise from the same species because they decay with similar rates (see later). The CO_2-induced bands connected with the presence of *cis*-FA are shown in Table 2, and they are assigned to the *cis*-FA···CO_2 complex.

As shown in trace 4 in Figure 3, the *cis*-FA monomer disappears almost completely after 1 h in the dark whereas the *cis*-FA···CO_2 complex bands are still present in the spectrum. Trace 5 in Figure 3 is a difference spectrum showing the result of 19 h in the dark with respect to trace 4. The group of bands III slowly decreases in intensity whereas the *trans*-FA···CO_2 complex (band II) is formed. Some formation of band I is also observed although it is about 1 order of magnitude weaker than band II.

Figure 4 presents the decays of the *cis*-FA···CO_2 complex and *cis*-FA monomer obtained by integrating the corresponding

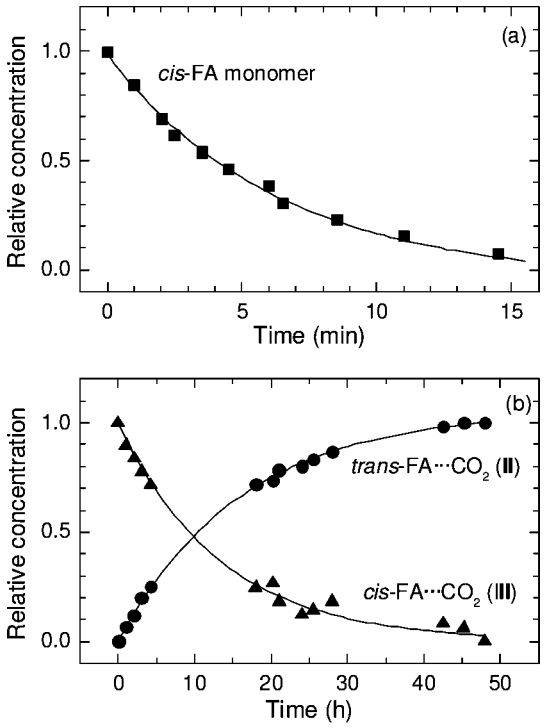

Figure 4. Relative concentrations of (a) *cis*-FA monomer and (b) *cis*-FA···CO_2 complex **III** and *trans*-FA···CO_2 complex **II** as a function of the time at 10 K.

C═O stretching bands. By fitting the decay with a single exponential function, the lifetimes of *cis*-FA monomer and *cis*-FA···CO_2 complex at 10 K are determined to be 6.3 min and 13.3 h, respectively. The formation of the *trans*-FA···CO_2 complex (Figure 4b) is fitted by an exponential association function $(1 - e^{-t/\tau})$ with the lifetime of 16.2 h. The *cis*-FA···CO_2 bands in the deformation region decay with lifetimes of 18.0 h (1274.7 cm^{-1}), 16.3 h (1258.3 and 1256.4 cm^{-1}), 14.4 h (1251.6 and 1249.7 cm^{-1}), and 13.9 h (1245.3 cm^{-1}). The decay rate increases with the temperature and the decays of *cis*-FA···CO_2 complex at 10, 20, and 30 K are shown in Figure S1. The lifetimes of the monomer and complex are about 2 min and 8 h at 20 K, and about 1 min and 2 h at 30 K. The present data for the *cis*-FA monomer agree with the detailed data reported previously.[15,18]

DISCUSSION

Spectral Assignment. The CO_2-induced bands observed in the deposited matrix containing only the *trans* conformer are divided into two groups I and II based on their behavior upon annealing at 30 K. The bands that increase upon annealing (group I) are assigned to the *trans*-FA···CO_2 complex **I** and the decreasing bands (group II) are assigned to the *trans*-FA···CO_2 complex **II** (see Figure 3 and Table 1).

The experimental frequency shifts of the *trans*-FA···CO_2 complex **I** agree well with the calculated values (Table 1). The νOH, νC═O, COH−CO deformation, and τCOH bands of the *trans*-FA···CO_2 complex **I** are shifted from the *trans*-FA monomer bands, respectively, by −45.0, −12.1, +22.2, and +54.0 cm^{-1} in the experiment and by −57.7, −12.1, +30.2, and

dx.doi.org/10.1021/jp302911p | J. Phys. Chem. A 2012, 116, 5305−5311

+81.3 cm^{-1} in the calculations. For the CO−COH deformation mode, we cannot compare the experimental and computational shifts accurately because this *trans*-FA mode is split by Fermi resonance with the first overtone of the torsion mode whereas the CO−COH deformation of the *trans*-FA···CO_2 complex is free from Fermi resonance. However, the averaged shift from the Fermi components is consistent with the calculated value of +20.3 cm^{-1}. The appearance of *four* bands for the CO−COH deformation mode is probably due to a matrix site effect. After annealing of the as-deposited matrix, the relative intensities of these bands change, and the highest frequency band at 1280.0 cm^{-1} becomes relatively stronger than the others (traces 1 and 2 in Figure 3). These bands can also be contributed by the symmetric stretching mode of carbon dioxide in complex **I**, which becomes IR active upon complex formation although the calculated IR intensity of this mode (4 km mol^{-1}) is weaker than that of the CO−COH deformation mode (12 km mol^{-1}). Experiments with $C^{18}O_2$ isotopomer can in principle shed light on this question. Other absorptions of carbon dioxide in the complex are not found presumably due to the minor shifts from the monomer.

For the *trans*-FA···CO_2 complex **II**, the agreement between the experiment and theory is also acceptable; the νOH, νC═O, and τCOH modes are shifted, respectively, by −4.0, −5.8, and −7.2 cm^{-1} in the experiment and by −2.4, +0.9, and −0.8 cm^{-1} in the calculations. It should be noted that the calculations are done for the species in vacuum whereas the experiment is performed in solid argon. Interaction with the surrounding argon atoms can change the geometry of weakly bound complexes and consequently change the spectra.

The *cis*-FA···CO_2 complexes are prepared by vibrational excitation of *trans*-FA and simultaneous annealing of an FA/CO_2/Ar matrix. The vibrational excitation produces *cis*-FA and annealing leads to the formation of the *cis*-FA···CO_2 complexes. This strategy has been previously used to prepare the *cis*-FA···H_2O, *cis*-FA···N_2, and *cis*-FA···O complexes and trans−cis and cis−cis FA dimers.[16,20,21,24,25] The bands assigned to the *cis*-FA···CO_2 complex **III** appear in the spectra only when annealing is applied to a matrix containing simultaneously CO_2 and *cis*-FA.

The experimental frequency shifts of the *cis*-FA···CO_2 complex **III** agree well with the calculated values. For example, the νOH and νC═O bands of *cis*-FA are shifted by −15.4 and −6.7 cm^{-1} in the experiment and by −18.0 and −4.9 cm^{-1} in the calculations (Table 2). The CO−COH deformation mode is split to seven bands, which may be due to a matrix site effect, similarly to the case of the *trans*-FA···CO_2 complex. It is improbable that some of these bands originate from the symmetric stretching mode of CO_2 because the calculated IR intensity of this mode for complex **III** (8 km mol^{-1}) is much weaker than that of the CO−COH deformation mode (270 km mol^{-1}). The COH−CO deformation band of the *cis*-FA···CO_2 complex is not found probably due to an overlap with the corresponding band of the *trans*-FA monomer and *trans*-FA···CO_2 complex. The asymmetric stretching and bending bands of complexed CO_2 are not observed probably due to their small shifts from the monomeric bands.

No evidence for the formation of the *cis*-FA···CO_2 complex **IV** has been found in the spectra. It is notable that the calculated shift of the CO−COH deformation mode (−1.8 cm^{-1}) is close to the experimental shifts for some of the *cis*-FA···CO_2 complex bands (−3.4 to +8.4 cm^{-1}) (see Table 2). However, similar decay rates for the seven bands observed in this region indicate that they originate from similar structures. Most probably, complex **IV** should decay much faster than complex **III** as suggested by the calculated stabilization barriers. It is possible that complex **IV** decays very fast upon annealing, hence escaping from the observation. The lack of complex **IV** is also consistent with its smaller interaction energy as compared to complex **III**. Similarly, only the H-bonded complex has been identified in the case of *cis*-FA···N_2 complex.[21] Indeed, the combination of vibrational excitation and annealing used here is more suitable for the preparation of stable systems.

Tunneling Reaction. It is shown in Figure 4 that the decay of the *cis*-FA···CO_2 complex (τ = 13.3 h) is much slower than that of the *cis*-FA monomer (τ = 6.3 min). *cis*-FA decays by tunneling of the hydrogen atom through the torsional barrier,[11] and the decay of the *cis*-FA···CO_2 complex **III** presumably occurs by the same mechanism. It has been suggested that several factors, such as the barrier height, solvation effect, coupling between vibrational levels, and the nature of the accepting mode can affect the tunneling rate.[15,26] However, the torsional barrier is evidently the most important factor controlling the cis-to-trans conversion of carboxylic acids.[11]

Figure 2 presents the calculated torsional barriers for the cis-to-trans conversion of the *cis*-FA monomer and *cis*-FA···CO_2 complex **III**, the barrier heights in vacuum being 3242 and 4161 cm^{-1}, respectively. This difference (919 cm^{-1} = 10.9 kJ mol^{-1}) mainly originates from the interaction energy of the *cis*-FA···CO_2 complex **III** (−9.9 kJ mol^{-1}). The higher barrier in complex **III** makes its decay slower compared with the *cis*-FA monomer, in agreement with the experimental results.

Interaction with the matrix affects the energetics of the system.[15] The PCM model shows that the barrier in solid argon increases by 126 cm^{-1} (∼5%) for the monomer but decreases by 178 cm^{-1} (∼7%) for complex **III** as compared to the vacuum case. Although these changes should be considered qualitatively, the solvation in argon matrix tends to decrease the difference in lifetimes of the *cis*-FA···CO_2 complex and *cis*-FA monomer.

The differences of the lifetimes of these species can be estimated using the Wentzel−Kramers−Brillouin (WKB) approximation.[34] In this approximation, the transmission coefficient of the barrier is given as

$$T = \frac{\exp\left(-2\int_{x_1}^{x_2} dx \sqrt{\frac{2m}{\hbar^2}(V(x) - E)}\right)}{\left(1 + \frac{1}{4}\exp\left(-2\int_{x_1}^{x_2} dx \sqrt{\frac{2m}{\hbar^2}(V(x) - E)}\right)\right)^2} \quad (1)$$

where x_1 and x_2 are the boundaries of the potential barrier, m is the mass of the tunneling particle, $V(x)$ is the potential energy, and E is the energy of the tunneling particle. By using the calculated torsional barriers in vacuum, the transmission coefficients are estimated to be 4.6×10^{-18} and 2.7×10^{-22} for the *cis*-FA monomer and *cis*-FA···CO_2 complex **III**, respectively; i.e., their ratio exceeds 10^4. When solvation is taken into account, the transmission coefficients become 1.0×10^{-18} and 2.3×10^{-21} for the monomer and complex, respectively, whose ratio (∼400) reasonably agrees with the ratio of the experimental lifetimes (∼130).

The temperature dependence of decay rates of the *cis*-FA monomer is well-known.[15,18] The decay rate becomes faster at higher temperatures and it reaches the low temperature limit at about 10 K. The existence of low temperature limit, together with the huge isotope effect, is characteristic of tunneling

dx.doi.org/10.1021/jp302911p | J. Phys. Chem. A 2012, 116, 5305−5311

reactions.[35] The lifetime of *cis*-FA···CO_2 complex **III** is about 13.3, 8, and 2 h at 10, 20, and 30 K, respectively. This dependence is similar to that of the *cis*-FA monomer. The temperature dependence of tunneling reactions has a very complex mechanism, where the medium reorganization plays an important role.[36]

It is worth comparing the *cis*-FA···CO_2 complex **III** with the H-bonded complexes *cis*-FA···H_2O and *cis*-FA···N_2.[20,21] The *cis*-FA···H_2O complex is absolutely stable on the scale of days at low temperatures and the *cis*-FA···N_2 complex decays at 9 K with a lifetime of ca. 48 min. The stability of the *cis*-FA···H_2O complex is explained by the strong OH···OH_2 hydrogen bond (interaction energy of −32.0 kJ mol^{-1}). Because the *cis*-FA···H_2O complex is lower in energy than the *trans*-FA + H_2O pair, the cis-to-trans conversion in this complex is impossible within the adiabatic approximation. The interactions in the *cis*-FA···N_2 and *cis*-FA···CO_2 complexes are weaker, which allows the cis-to-trans conversion. The calculated barrier for the *cis*-FA···N_2 complex is 3715 cm^{-1},[21] which is between the values of the *cis*-FA monomer (3242 cm^{-1}) and *cis*-FA···CO_2 complex (4161 cm^{-1}). These calculated values agree with the order of the experimental lifetimes.

Finally, we comment on the conversion process of complex **III**. It is found that the *trans*-FA···CO_2 complex **II** is mainly formed during the decay of the *cis*-FA···CO_2 complex **III**. The decay time of complex **III** (τ = 13.3 h and from 13.9 to 18.0 h measured in the C═O stretching and deformation regions, respectively) is very similar to the formation time of complex **II** (τ = 16.2 h). These results imply that the cis-to-trans conversion in the *cis*-FA···CO_2 complex **III** leads preferably to the formation of complex **II**. The proposed mechanism is illustrated in Scheme 1. Hydrogen tunneling occurs on a short

Scheme 1

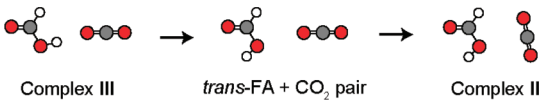

time scale, and the reorganization of heavy atoms does not occur during the tunneling time (adiabatic approximation).[31] Therefore, the cis-to-trans conversion of complex **III** leads to the formation of a *trans*-FA + CO_2 pair, and this unstable structure then relaxes mainly to complex **II** at a longer time scale. It is not a surprise that a small amount of complex **I** is produced in this process at 10 K because it is the most stable structure of the *trans*-FA···CO_2 complex. The decay at 20 K generates much larger amount of complex **I** as compared to complex **II**, and complex **II** is not observed in the decay at 30 K. These results indicate that the conversion rate of complex **II** to complex **I** is strongly enhanced at elevated temperatures.

CONCLUSIONS

Two *trans*-FA···CO_2 and two *cis*-FA···CO_2 complexes are obtained theoretically (Figure 1). Their geometries, interaction energies, vibrational spectra are obtained by ab initio calculations at the MP2(full)/6-311++G(2d,2p) level of theory. Two *trans*-FA···CO_2 (**I** and **II**) and one *cis*-FA···CO_2 (**III**) complexes are identified by infrared spectroscopy in solid argon (Tables 1 and 2). The experimental complexation-induced frequency shifts agree with the calculated values, allowing reliable structural assignment.

The *trans*-FA···CO_2 complexes **I** and **II** are observed in argon matrixes after deposition at 10 K. The less stable *trans*-FA···CO_2 complex **II** disappears upon annealing of the matrix at about 30 K, probably converting to the more stable structure **I**. The H-bonded *cis*-FA···CO_2 complex **III** is prepared by vibrational excitation of *trans*-FA and simultaneous annealing of the FA/CO_2/Ar matrix. The *cis*-FA···CO_2 complex **III** decays in the dark with a lifetime of about 13 h whereas the *cis*-FA monomer decays much faster with a lifetime of about 6 min (Figure 4). The decay of the *cis*-FA···CO_2 complex **III** at the lowest temperature leads mainly to the formation of the *trans*-FA···CO_2 complex **II** (Scheme 1). Complex **IV** has not been identified, which is probably connected with a lower stabilization barrier and/or weaker interaction in this structure.

The decay of the H-bonded *cis*-FA···CO_2 complex is 130 times slower than that of the *cis*-FA monomer. This remarkable difference can be explained in terms of torsional barriers for the cis-to-trans conversion, taking into account the solvation effects. The calculations predict that the torsional barrier of *cis*-FA···CO_2 complex is higher than that of the *cis*-FA monomer by about 900 cm^{-1} (in vacuum) explaining the observed stabilization of the higher-energy conformer in the complex. The solvation in solid argon decreases the difference of these barriers by about 300 cm^{-1}. The estimates based on the WKB approximation yield reasonable agreement with the experiment for the lifetimes of the complex and monomer, especially after taking solvation into account.

ASSOCIATED CONTENT

Supporting Information

Decays of *cis*-FA···CO_2 complex **III** at 10, 20, and 30 K (Figure S1) and complete refs 8 and 29. This material is available free of charge via the Internet at http://pubs.acs.org.

AUTHOR INFORMATION

Corresponding Author

*E-mail: (M.T.) masashi.tsuge@helsinki.fi; (L.K.) leonid.khriachtchev@helsinki.fi.

Notes

The authors declare no competing financial interest.

ACKNOWLEDGMENTS

This work was supported by the Academy of Finland through the Finnish Centre of Excellence in Computational Molecular Science and Grant 139105. CSC−IT Center for Science Ltd. is thanked for computational resources.

REFERENCES

(1) Robertson, E. G.; Simons, J. P. *Phys. Chem. Chem. Phys.* **2001**, *3*, 1−18.
(2) Baldeschwieler, J. D.; Pimentel, G. C. *J. Chem. Phys.* **1960**, *33*, 1008−1015.
(3) Qin, Y.; Thompson, D. L. *J. Chem. Phys.* **1994**, *100*, 6445−6457.
(4) Akai, N.; Kudoh, S.; Nakata, M. *J. Phys. Chem. A* **2003**, *107*, 3655−3659.
(5) Nanbu, S.; Sekine, M.; Nakata, M. *J. Phys. Chem. A* **2011**, *115*, 9911−9918.
(6) Zuev, P. S.; Sheridan, R. S.; Albu, T. V.; Truhlar, D. G.; Hrovat, D. A.; Borden, W. T. *Science* **2003**, *299*, 867−870.
(7) Schreiner, P. R.; Reisenauer, H. P.; Ley, D.; Gerbig, D.; Wu, C.-H.; Allen, W. D. *Science* **2011**, *332*, 1300−1303.
(8) Neill, J. L.; Steber, A. L.; Muckle, M. T.; Zaleski, D. P.; Lattanzi, V.; Spezzano, S.; McCarthy, M. C.; Remijan, A. J.; Friedel, D. N.; Widicus Weaver, S. L.; et al. *J. Phys. Chem. A* **2011**, *115*, 6472−6480.

(9) McMahon, R. J. *Science* **2003**, *299*, 833−834.
(10) Hiraoka, K.; Sato, T.; Takayama, T. *Science* **2001**, *292*, 869−870.
(11) Khriachtchev, L. *J. Mol. Struct.* **2008**, *880*, 14−22.
(12) Hocking, W. H. Z. *Naturforsch. A* **1976**, *31a*, 1113−1121. Our notation of the trans and cis conformers of FA follows this reference although the opposite notation can be found in the literature.
(13) Pettersson, M.; Lundell, J.; Khriachtchev, L.; Räsänen, M. *J. Am. Chem. Soc.* **1997**, *119*, 11715−11716.
(14) Pettersson, M.; Maçôas, E. M. S.; Khriachtchev, L.; Fausto, R.; Räsänen, M. *J. Am. Chem. Soc.* **2003**, *125*, 4058−4059.
(15) Pettersson, M.; Maçôas, E. M. S.; Khriachtchev, L.; Lundell, J.; Fausto, R.; Räsänen, M. *J. Chem. Phys.* **2002**, *117*, 9095−9098.
(16) Khriachtchev, L.; Domanskaya, A.; Marushkevich, K.; Räsänen, M.; Grigorenko, B.; Ermilov, A.; Andrijchenko, N.; Nemukhin, A. *J. Phys. Chem. A* **2009**, *113*, 8143−8146.
(17) Lopes, S.; Domanskaya, A. V.; Fausto, R.; Räsänen, M.; Khriachtchev, L. *J. Chem. Phys.* **2010**, *133*, 144507.
(18) Marushkevich, K.; Khriachtchev, L.; Räsänen, M. *J. Chem. Phys.* **2007**, *126*, 241102.
(19) Marushkevich, K.; Khriachtchev, L.; Räsänen, M. *Phys. Chem. Chem. Phys.* **2007**, *9*, 5748−5751.
(20) Marushkevich, K.; Khriachtchev, L.; Räsänen, M. *J. Phys. Chem. A* **2007**, *111*, 2040−2042.
(21) Marushkevich, K.; Räsänen, M.; Khriachtchev, L. *J. Phys. Chem. A* **2010**, *114*, 10584−10589.
(22) Marushkevich, K.; Khriachtchev, L.; Lundell, J.; Räsänen, M. *J. Am. Chem. Soc.* **2006**, *128*, 12060−12061.
(23) Marushkevich, K.; Khriachtchev, L.; Lundell, J.; Domanskaya, A.; Räsänen, M. *J. Phys. Chem. A* **2010**, *114*, 3495−3502.
(24) Marushkevich, K.; Siltanen, M.; Räsänen, M.; Halonen, L.; Khriachtchev, L. *J. Phys. Chem. Lett.* **2011**, *2*, 695−699.
(25) Maruchkevich, K.; Khriachtchev, L.; Räsänen, M.; Melavuori, M.; Lundell, J. *J. Phys. Chem. A* **2012**, *116*, 2101−2108.
(26) Domanskaya, A.; Marushkevich, K.; Khriachtchev, L.; Räsänen, M. *J. Chem. Phys.* **2009**, *130*, 154509.
(27) Tielens, A. G. G. M.; Allamandola, L. J. In *Physics and Chemistry at Low Temperatures*; Khriachtchev, L., Ed.; Pan Stanford Publishing: Singapore, 2011; pp 341−380.
(28) Hull, J. F.; Himeda, Y.; Wang, W.-H.; Hashiguchi, B.; Periana, R.; Szalda, D. J.; Muckerman, J. T.; Fujita, E. *Nature Chem.* **2012**, *4*, 383−388.
(29) Frisch, M. J.; Trucks, G. W.; Schlegel, H. B.; Scuseria, G. E.; Robb, M. A.; Cheeseman, J. R.; Scalmani, G.; Barone, V.; Mennucci, B.; Petersson, G. A. et al. *Gaussian 09*, Revision A.01. Gaussian, Inc.: Wallingford CT, 2009.
(30) Boys, S. F.; Bernardi, F. *Mol. Phys.* **1970**, *19*, 553−566.
(31) Trakhtenberg, L. I. In *Atom Tunneling Phenomena in Physics, Chemistry and Biology*; Miyazaki, T., Ed.; Springer-Verlag: Berlin, 2004; pp 33−58.
(32) Tomasi, J.; Mennucci, B.; Cammi, R. *Chem. Rev.* **2005**, *105*, 2999−3093.
(33) Maçôas, E. M. S.; Lundell, J.; Pettersson, M.; Khriachtchev, L.; Fausto, R.; Räsänen, M. *J. Mol. Spectrosc.* **2003**, *219*, 70−80.
(34) Razavy, M. *Quantum Theory of Tunneling*; World Scientific: Singapore, 2003; pp 23−31.
(35) Goldanskii, V. I.; Frank-Kamenetskii, M. D.; Barkalov, I. M. *Science* **1973**, *182*, 1344−1345.
(36) Ivanov, G. K.; Kozhushner, M. A.; Trakhtenberg, L. I. *J. Chem. Phys.* **2000**, *113*, 1992−2002.